

## Article

# De-Emulsification and Gravity Separation of Micro-Emulsion Produced with Enhanced Oil Recovery Chemicals Flooding

Mohammad Kamal Asif Khan <sup>1,\*</sup>, Javed Akbar Khan <sup>2,\*</sup>, Habib Ullah <sup>3</sup>, Hussain H. Al-Kayiem <sup>2</sup>,  
Sonny Irawan <sup>4</sup>, Muhammad Irfan <sup>5</sup>, Adam Glowacz <sup>6,\*</sup>, Hui Liu <sup>7</sup>, Witold Glowacz <sup>6</sup>  
and Saifur Rahman <sup>5</sup>

- <sup>1</sup> Mechanical Engineering Department, College of Engineering, Najran University, Najran 61441, Saudi Arabia
  - <sup>2</sup> Mechanical Engineering Department, Universiti Teknologi PETRONAS, Seri Iskandar 32610, Malaysia; hussain\_kayiem@utp.edu.my
  - <sup>3</sup> Fundamental and Applied Sciences Department, Universiti Teknologi PETRONAS, Seri Iskandar 32610, Malaysia; habibullah\_kust@yahoo.com
  - <sup>4</sup> School of Mining & Geosciences, Nazarbayev University, Nur-Sultan City 010000, Kazakhstan; irawan.sonny@nu.edu.kz
  - <sup>5</sup> Electrical Engineering Department, College of Engineering, Najran University, Najran 61441, Saudi Arabia; miditta@nu.edu.sa (M.I.); srrahman@nu.edu.sa (S.R.)
  - <sup>6</sup> Department of Automatic Control and Robotics, Faculty of Electrical Engineering, Automatics, Computer Science and Biomedical Engineering, AGH University of Science and Technology, Al. A. Mickiewicza 30, 30-059 Kraków, Poland; wglowacz@agh.edu.pl
  - <sup>7</sup> College of Quality and Safety Engineering, China Jiliang University, Hangzhou 310018, China; hui.liu@cjl.u.edu.cn
- \* Correspondence: mkkhan@nu.edu.sa (M.K.A.K.); javedkhan\_niazi@yahoo.com (J.A.K.); adglow@agh.edu.pl (A.G.)



**Citation:** Khan, M.K.A.; Khan, J.A.; Ullah, H.; Al-Kayiem, H.H.; Irawan, S.; Irfan, M.; Glowacz, A.; Liu, H.; Glowacz, W.; Rahman, S. De-Emulsification and Gravity Separation of Micro-Emulsion Produced with Enhanced Oil Recovery Chemicals Flooding. *Energies* **2021**, *14*, 2249. <https://doi.org/10.3390/en14082249>

Academic Editor: Mahmood Reza Yassin

Received: 9 March 2021

Accepted: 14 April 2021

Published: 16 April 2021

**Publisher's Note:** MDPI stays neutral with regard to jurisdictional claims in published maps and institutional affiliations.



**Copyright:** © 2021 by the authors. Licensee MDPI, Basel, Switzerland. This article is an open access article distributed under the terms and conditions of the Creative Commons Attribution (CC BY) license (<https://creativecommons.org/licenses/by/4.0/>).

**Abstract:** The present study investigates the effect of TiO<sub>2</sub> nanoparticles on the stability of Enhanced Oil Recovery (EOR)-produced stable emulsion. The chemical precipitation method is used to synthesize TiO<sub>2</sub> nanoparticles, and their properties were determined using various analytical characterization techniques such as X-ray Diffraction (XRD), High-Resolution Transmission Electron Microscopy (HRTEM), and Field Emission Scanning Electron Microscopy (FESEM). The effect of TiO<sub>2</sub> nanoparticles is evaluated by measuring oil/water (o/w) separation, rag layer formation, oil droplet size, and zeta potential of the residual EOR produced emulsion. The laser scattering technique is used to determine the o/w separation. The results showed that spherical-shaped anatase phase TiO<sub>2</sub> nanoparticles were produced with an average particle size of 122 nm. The TiO<sub>2</sub> nanoparticles had a positive effect on o/w separation and the clarity of the separated water. The separated aqueous phases' clarity is 75% and 45% with and without TiO<sub>2</sub> nanoparticles, respectively. Laser scattering analysis revealed enhanced light transmission in the presence of TiO<sub>2</sub> nanoparticles, suggesting higher o/w separation of the ASP-produced emulsion. The overall increase in the o/w separation was recorded to be 19% in the presence of TiO<sub>2</sub> nanoparticles, indicating a decrease in the stability of ASP-produced emulsion. This decrease in the stability can be attributed to the improved coalescence' action between the adjacent oil droplets and improved behavior of o/w interfacial film. An observable difference was found between the oil droplet size before and after the addition of TiO<sub>2</sub> nanoparticles, where the oil droplet size increased from 3 µm to 35 µm. A similar trend of zeta potential is also noticed in the presence of TiO<sub>2</sub> nanoparticles. Zeta potential was −13 mV to −7 mV, which is in the unstable emulsion range. Overall, the o/w separation is enhanced by introducing TiO<sub>2</sub> nanoparticles into ASP-produced stable emulsion.

**Keywords:** EOR flooding; emulsification; gravity separation; laser scattering

## 1. Introduction

Many oilfield around the world are using flooding by Alkali/Surfactant/Polymer (ASP) to enhance the recovery of oil by as much as 20% as compared to water flooding. ASP flooding produces stable emulsion, decreasing the efficiency of gravity separation, and is considered one of the crucial limitations of flooding technology. An o/w emulsion is produced when the oil droplets, in the presence of an emulsifier, mix with water. The lower the oil concentration in the produced emulsion, the higher the emulsion stability [1]. Moreover, in the mass oil phase, dispersion of the water phase begins in the form of fine droplets. Figure 1 schematically describes the high shear zone occurring in the production system and forming in the emulsion.

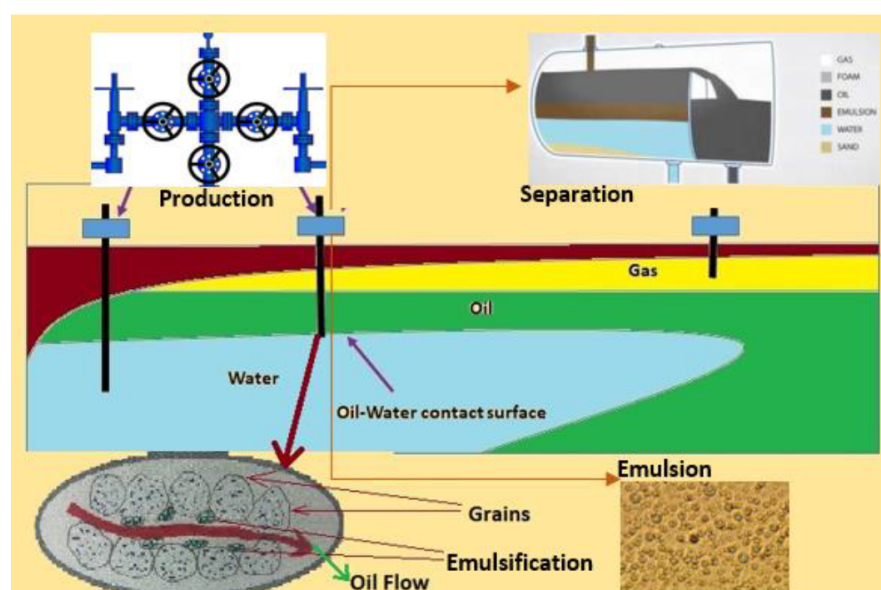


Figure 1. Phenomena of emulsification at production facility

When the droplet size in the emulsion is smaller than  $10\ \mu\text{m}$ , it would not be separated by gravitational force and, therefore, it needs to be separated by some other means. A previous study has reported that facility sites of oil fields are experiencing fluid transport problems due to the production of a high amount of crude oil in water, which makes a very stable o/w emulsion in the presence of ASP chemicals [2]. Studies have also reported high stability, higher emulsification, strong interfacial film strength, and a high content of small oil droplets in o/w emulsion [3,4]. Consequently, it is challenging to separate o/w, which significantly hinders the commercialized application of ASP flooding technology. According to Norman et al. [5], for the processing of oil in the downstream operations and its export in the crude form, o/w separation has an important role to play. For this reason, a metastable emulsion is a necessity for mobility improvement.

A good number of conventionally available techniques have been under investigation for the treatment of water produced in the oil fields, including, but not limited to, de-emulsification [6], gravity separation [7], membrane separation [8], floatation [9], adsorptive separation [10], air floatation [11], and bioprocesses [12]. However, the reports regarding the treatment of ASP flooding-produced water are rare in the literature. Only a few research groups have studied the o/w separation in ASP flooding-produced water. For instance, the investigation of increased downstream turbulence inside circular pipes through a circular orifice by Zande et al. [13] found an increase in the breakup of oil droplets in this condition. Similarly, an increase in the choking level at the inlet of the pipes and an increase in the surfactant quantity decreases the separator efficiency [14]. Deng et al. [15] removed the stable oil droplets in the produced water through flocculation and de-emulsification. Their findings suggested a better performance for oil-soluble de-emulsifier compared to a water-soluble de-emulsifier. However, these processes are costly

and need high capital investment. Moreover, according to Zonglin Chu et al. [16], a large number of studies have reported that the separation experiments were done with gasoline or pure oily liquid. This is very different to the actual oil pollutant present in any offshore oil pollution accident. The use of environmentally friendly materials and a cost-effective method is important and is required for sustainable applications in o/w separation [17,18]. Recently, a predictive model has been developed to assess the effectiveness of separation of o/w emulsion with ASP [19]. Various studies have been carried out to overcome the nonproductive time during upstream operations [20,21]. Such a study is required for downstream equipment, especially in the primary separator, as choking of separation processes results in the disturbance of flow assurance in the supply chain.

The development of nanoparticles with the desired properties and investigating their efficacy in the separation process has gained enormous research interest due to their ability to enhance the separation of o/w emulsion. Titanium dioxide ( $\text{TiO}_2$ ) nanoparticles are touted as a better option to enhance o/w separation because of their nano-size, excellent thermal and chemical stability, larger surface area, and cost-effectiveness [22]. For instance, Shi et al. [23] reported 99% separation of o/w mixture using  $\text{TiO}_2$  and copper wire mesh.  $\text{TiO}_2$  nanoparticles have shown a remarkable enhancement performance near critical micelle concentration conditions in the oil recovery process [24]. It has shown enhanced oil recovery performance and has a striking flow behavior in the heavy oil recovery process compared to base polymers [25]. Furthermore,  $\text{TiO}_2$  nanoparticles change the wettability from oil-wet to water-wet compared to other metal oxides nanoparticles [26–28]. So far, the nanomaterials have shown excellent potential for destabilization and o/w separation in ASP-produced emulsion.

The main purpose of the present work is to destabilize and remove oil from water in the ASP-produced stable emulsion. The effect of  $\text{TiO}_2$  nanoparticles on o/w separation in ASP-produced stable emulsions is investigated. The o/w separation and stability were monitored by measuring the oil and water content, droplet size, and zeta potential of the ASP emulsion before and after the addition of  $\text{TiO}_2$  nanoparticles. The  $\text{TiO}_2$  nanoparticles were synthesized via the chemical precipitation method using Titanium Tetrachloride ( $\text{TiCl}_4$ ) as a precursor. The characterization of the obtained  $\text{TiO}_2$  nanoparticles was done using X-ray Diffraction (XRD), Field Emission Scanning Electron Microscopy (FESEM), and High-Resolution Transmission Electron Microscopy (HRTEM). A different ASP is used to produce water in oil emulsion. As reported in the previous studies [2,29,30], the most stable emulsion was selected based on the primary separator's recorded breakthrough amount. The stability of the emulsion is determined using a Turbiscan (laser transmission and backscattering) device. Calculation of the o/w separation is done based on the aqueous phase sedimentation and the oil phase coalescence. The novelty of the present work is that the effect of  $\text{TiO}_2$  nanoparticles is evaluated on actual ASP-produced emulsion as opposed to previous studies, which were performed on model or synthetic emulsions. The main contribution of the present work is a remarkable 19% increase in o/w separation achieved in the presence of  $\text{TiO}_2$  nanoparticles, which indicates that the stability of the ASP-produced emulsion is significantly destabilized. The separated water clarity comes out to be 75% against 45% with and without  $\text{TiO}_2$  nanoparticles, respectively. This study corroborated that the  $\text{TiO}_2$  nanoparticles have considerably destabilized the emulsion and exhibited a considerable potential for separation enhancement for ASP-produced emulsion. The present work will support the separation and treatment processes in the fields where EOR is under execution.

## 2. Materials and Methods

The materials used in the emulsion are crude oil, brine, and ASP. Sodium-Carbonate ( $\text{Na}_2\text{CO}_3$ ), Anionic Alpha Olefin Sulfonate (AOS) (CMC 0.10 (wt% AOS) with the structural formula  $\text{RCH}(\text{OH})(\text{CH}_2)_n\text{SO}_3\text{Na}$  and anionic hydrolyzed polyacrylamide (PAM) with 16 (million Dalton) molecular weight were used as alkali, surfactant and polymer, respectively in the present study. The structural formula of surfactant is  $\text{RCH}(\text{OH})(\text{CH}_2)_n$

SO<sub>3</sub>Na. The chemicals used in this study were provided by PETRONAS Research Sdn Bhd, which uses these chemicals for EOR. The chemical breakthrough in the o/w gravity separator was used to obtain the ASP amount used in this work. Titanium tetrachloride (TiCl<sub>4</sub>, 99%) was purchased from Merck and was used as a precursor in preparing TiO<sub>2</sub> nanoparticles. Ammonium hydroxide (NH<sub>3</sub>OH, 30%) was used as a precipitating agent.

### 2.1. Preparation of Emulsion

The first step in the emulsion preparation is to prepare the aqueous solution of brine and ASP. Each component, Alkali (A), Surfactant (S), and Polymer (P), was homogeneously mixed in the aqueous phase. Secondly, before mixing/stirring the crude and brine with ASP composition, the solution of brine with ASP and crude oil was heated to attain the required temperature. The emulsion was produced by mixing 40% brine solution containing ASP with 60% oil, respectively, by mixing with a homogenizer (IKA T25) at 12,000 RPM for 2 min.

### 2.2. Preparation of TiO<sub>2</sub> Nanoparticles

For this study, the TiO<sub>2</sub> nanoparticles were prepared using the chemical precipitation technique. Typically, 0.1 moles of TiCl<sub>4</sub> was added dropwise to water (50 mL) under vigorous stirring in an ice bath. Then, NH<sub>4</sub>OH was added drop by drop to the resultant solution, and the precipitates were obtained at pH 10. The precipitates were rinsed several times in the distilled water to remove the residual chloride ions. The precipitates were recovered through centrifugation and dried at 60 °C for 36 h. Finally, the dried TiO<sub>2</sub> powder was calcined at 300 °C for 2 h.

### 2.3. Characterization of TiO<sub>2</sub> Nanoparticles

An X-ray Diffraction (XRD) spectrometer (PANalytical X'Pert<sup>3</sup> Powder, AA Almelo, The Netherlands) is used to determine the crystalline structure of the synthesized material. The XRD patterns of the synthesized TiO<sub>2</sub> nanoparticles was obtained in the range of 20 to 80° (2θ) using Cu-Kα irradiation (λ = 0.15406 nm) at room temperature with a 0.001° (2θ) of step size per second. High Resolution Transmission Electron Microscopy (HRTEM) analysis was performed in combination with XRD to differentiate disordered and amorphous phase from crystalline phase and get integrated information about the lattice parameters and nanoscale properties of the material. HRTEM micrographs of the samples were obtained using Tecnai G2-F20 X-Twin TMP Transmission Electron Microscope (NE Dawson Creek Drive, Hillsboro, OR, USA) equipped with Gatan Digital-Micrograph software (Pleasanton, CA, USA). Field Emission Scanning Electron Microscopy (FESEM) photographs of the samples were captured at 100 kX magnification and a working distance of 3–5 mm using Carl Zeiss instrument (SUPRA 55VP, Oberkochen, Germany) operated at a 20 kV of acceleration voltage.

### 2.4. Stability of Emulsion and Determination of Coalescence and Sedimentation

The stability test is important as it defines the separation of each phase (water and oil) in the emulsion. The bottle test is the most widely employed method to determine the stability of the emulsion. However, it is difficult to accurately measure the emulsion's stability using the bottle test [31,32]. Therefore, in the present study, the Turbiscan method is used to determine the stability of ASP emulsion more precisely and accurately as it is important to know the exact impact of the parameters under investigation. The Turbiscan device consists of two main components, namely, an optical scanning device, which works as a pulsed infrared (IR) light source, and a detector that is located opposite to the optical device or light source and it measures the transmittance of light through the glass vessel containing the emulsion sample. The Turbiscan device, by default, measures the transmittance of light and records it on the computer's hard disk. The percentage of water separated in the emulsion was determined at a specific interval of 10 min, 1, 2, 4, 10, 20

and 24 h. Figure 2 shows the schematic of the procedure used in the current study for measuring the light transmission and backscattering.

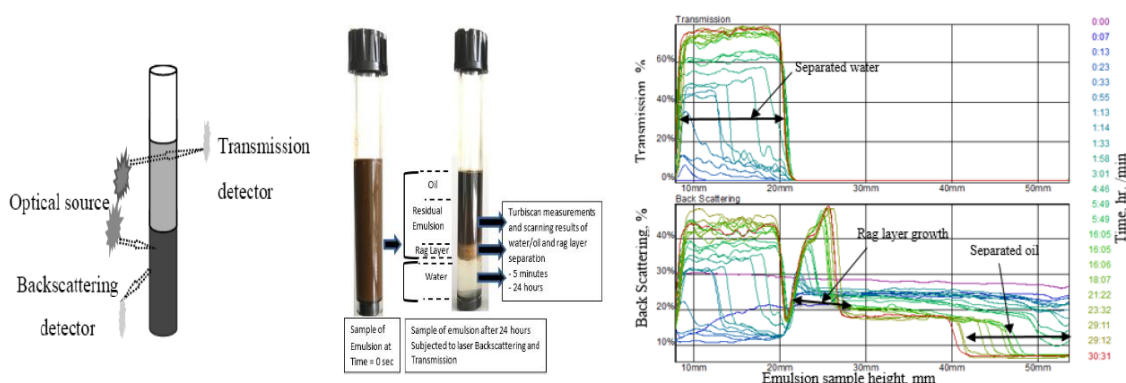


**Figure 2.** Schematic of the Tuberscan device for light measurements and experimental measurement of separation from emulsion sample; deliberate profiles of the transmission and backscattering rate for emulsion as a function of time.

The samples volume for the Turbiscan laser transmission and the scattering test were taken as 7 mL. The purpose of performing the Turbiscan test is that in the case of tricky observations in less clear fluid, it can calculate the o/w phases separated during the test. Thus, it assists in a rapid and sensitive approach to determine the emulsion stability. Again, an increase in the transmittance of light from the bottom of the test tube to the top determines the phases separation. This is done with the help of a scanning device and a glass vial containing the emulsion is scanned vertically with the device. Simultaneously, the change in light transmittance is recorded for the glass vial moving vertically upwards. Figure 2 shows that the laser scan of the kinetic curve results in the emulsion taken from the Turbiscan device at varying levels of additive concentrations. The measurements are carried out at a specific interval to find the sedimentation of the water phase and coalescence of oil phase. The sedimentation and coalescence heights are converted into separation percentages.

### 3. Results and Discussion

#### 3.1. Properties of the $\text{TiO}_2$ Nanoparticles

##### 3.1.1. Crystalline Structure

The XRD patterns of the synthesized  $\text{TiO}_2$  nanoparticles are shown in Figure 3. The XRD patterns of the  $\text{TiO}_2$  nanoparticles show a sharp diffraction peak at  $2\theta = 25.2^\circ$ , matching well with the (101) plane of the anatase phase. The  $\text{TiO}_2$  nanoparticles display only an anatase crystalline structure where the diffraction peaks detected at  $2\theta = 25.3^\circ, 37.9^\circ, 48.2^\circ, 54.1^\circ, 55.2^\circ, 63.0^\circ, 68.9^\circ, 70.5^\circ$ , and  $75.4^\circ$  were assigned to (101), (004), (200), (105), (211), (204), (116), (220), and (215) planes, respectively. No other diffraction peaks of rutile or brookite crystalline structures are detected in the diffraction patterns of the  $\text{TiO}_2$  nanoparticles, confirming that the sample is purely anatase, which is consistent with previous work [33].

The  $\text{TiO}_2$  nanoparticles average crystal size is calculated according to Debye–Scherer Equation

$$D = \frac{k\lambda}{B \cos\theta} \quad (1)$$

using the main intense XRD peak at  $\sim 25.2^\circ$  ( $2\theta$ ). The average crystallite size of the nanoparticles is determined to be 48 nm. The  $\text{TiO}_2$  nanoparticles showed 71.69% crystallinity. The crystallinity of the synthesized  $\text{TiO}_2$  nanoparticles is calculated according to Nara Komya methods using the following Equation [34].

$$\text{Crystallinity (\%)} = \frac{\text{Area of crystalline peaks}}{\text{Area of all peaks}} \times 100\% \quad (2)$$



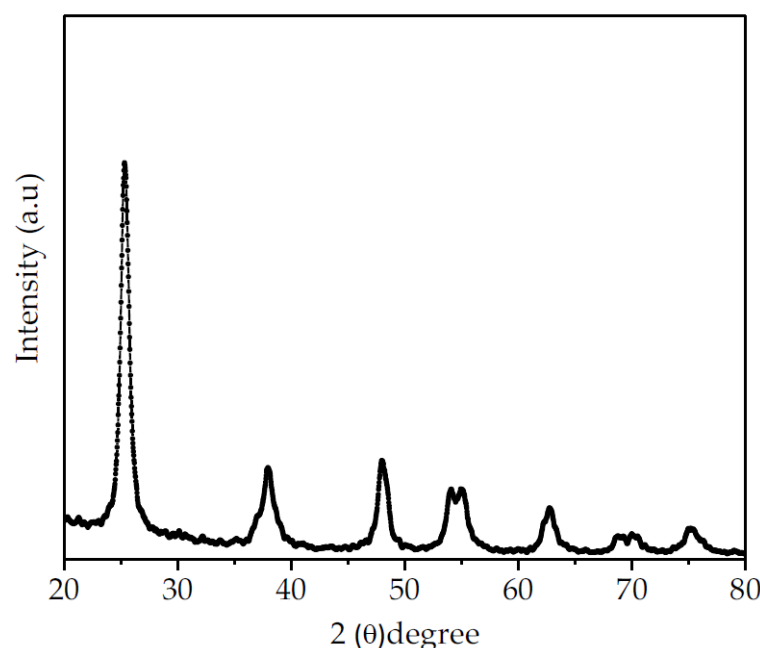


**Figure 3.** XRD patterns showing the anatase crystalline structure of the synthesized TiO<sub>2</sub> nanoparticles.

### 3.1.2. Surface Morphology

High Resolution Transmission Electron Microscopy (HRTEM) analysis is performed to get complementary information about the structural properties and surface morphology of the TiO<sub>2</sub> nanoparticles. The HRTEM imageries of the TiO<sub>2</sub> nanoparticles is presented in Figure 4a. The TiO<sub>2</sub> nanoparticles displayed well-resolved lattice features and clear lattice fringes. The distance between the two adjacent lattice planes of the TiO<sub>2</sub> nanoparticle was estimated by performing line analysis. From the distance between neighboring lattice fringes as shown in the inset of Figure 4a, the lattice spacing of distance (*d*) is 0.352 nm, which can be assigned to the inter-planar distance of the anatase (101) plane. This result is consistent with XRD and confirms that the TiO<sub>2</sub> nanoparticles are solely in the anatase phase. The Transmission Electron Microscopy (TEM) image in Figure 4b confirmed that the particles are well and truly nano-sized. The particle size distribution is estimated by measuring the diameter of 500 randomly selected particles from magnified HRTEM images using Image J software, developed by National Institutes of Health, Bethesda, MD, USA. A similar approach for estimating the particle size has also been reported by Yahaya et al. [35]. The particle size distribution of the synthesized TiO<sub>2</sub> nanoparticles was calculated based on Gaussian fitting and is presented in Figure 4d. Most of the nanoparticles were in the range of 80–160 nm, with an average particle size of 122 nm. The HRTEM image shows that the particles are predominantly spherical in shape, with a fraction of them spindle-shaped. The morphology of the TiO<sub>2</sub> nanoparticles was further investigated by FESEM. FESEM images were captured to obtain additional information on the morphology of the synthesized TiO<sub>2</sub> nanoparticles. An FESEM micrograph of the TiO<sub>2</sub> nanoparticle is shown in Figure 4c, which confirms that the spherical shape of particles is in good agreement with the HRTEM results.

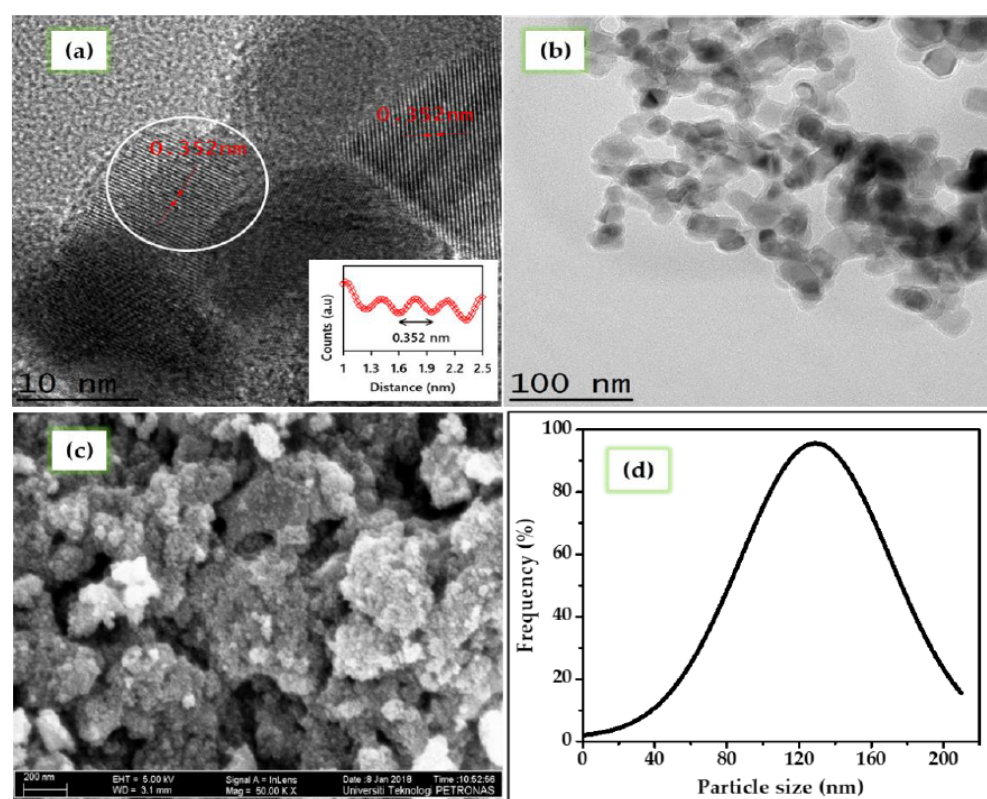


**Figure 4.** (a) High Resolution Transmission Electron Microscopy image (inset, result of line analysis), (b) Transmission Electron Microscopy Image, (c) Field Emission Scanning Electron Microscopy image, and (d) particle size distribution of the  $\text{TiO}_2$  nanoparticles.

### 3.2. ASP Emulsion Stability with and without $\text{TiO}_2$ Nanoparticles

It has been reported previously [2,29,30] that ASP produces a highly stable emulsion containing a residual oil-in-water phase which reduces separation efficiency because of the smaller oil droplet size. The most stable emulsion of ASP is selected, and the effect of  $\text{TiO}_2$  nanoparticles on the stability of the emulsion is investigated. A specific amount (300 mg/L) of  $\text{TiO}_2$  nanoparticles is added to the emulsion, and the stability is determined before and after the addition of the nanoparticles. The results of light transmission and backscattering of the ASP produced an emulsion with and without  $\text{TiO}_2$  nanoparticles are shown in Figure 5a,b, respectively. As can be seen from Figure 5a, the water layer is small; the rag layer is large in an ASP-produced emulsion without  $\text{TiO}_2$  nanoparticles. It is observed that the water layer increased while that of the residual emulsion decreased in the presence of  $\text{TiO}_2$  nanoparticles, as depicted in Figure 5b. Since  $\text{TiO}_2$  is intrinsically hydrophilic [36,37], it thus attracted the water molecules. A comparison of Figure 5a,b revealed that the light transmission has significantly increased in the presence of  $\text{TiO}_2$  nanoparticles. The light transmission was as low as 50% without  $\text{TiO}_2$  nanoparticles (Figure 4a) and 68% in the presence of  $\text{TiO}_2$  nanoparticles (Figure 5b). This can be attributed to the improved coalescence action between the adjacent oil droplets and the improved behavior of o/w interfacial film in the presence of  $\text{TiO}_2$  nanoparticles [38]. It can also be observed that backscattering was significantly reduced in the presence of  $\text{TiO}_2$  nanoparticles. The results indicate that the  $\text{TiO}_2$  nanoparticle has a significant effect on the o/w separation, which is consistent with a previous study which reported that  $\text{TiO}_2$  composite material acts as a promising de-emulsifier for o/w separation [39].

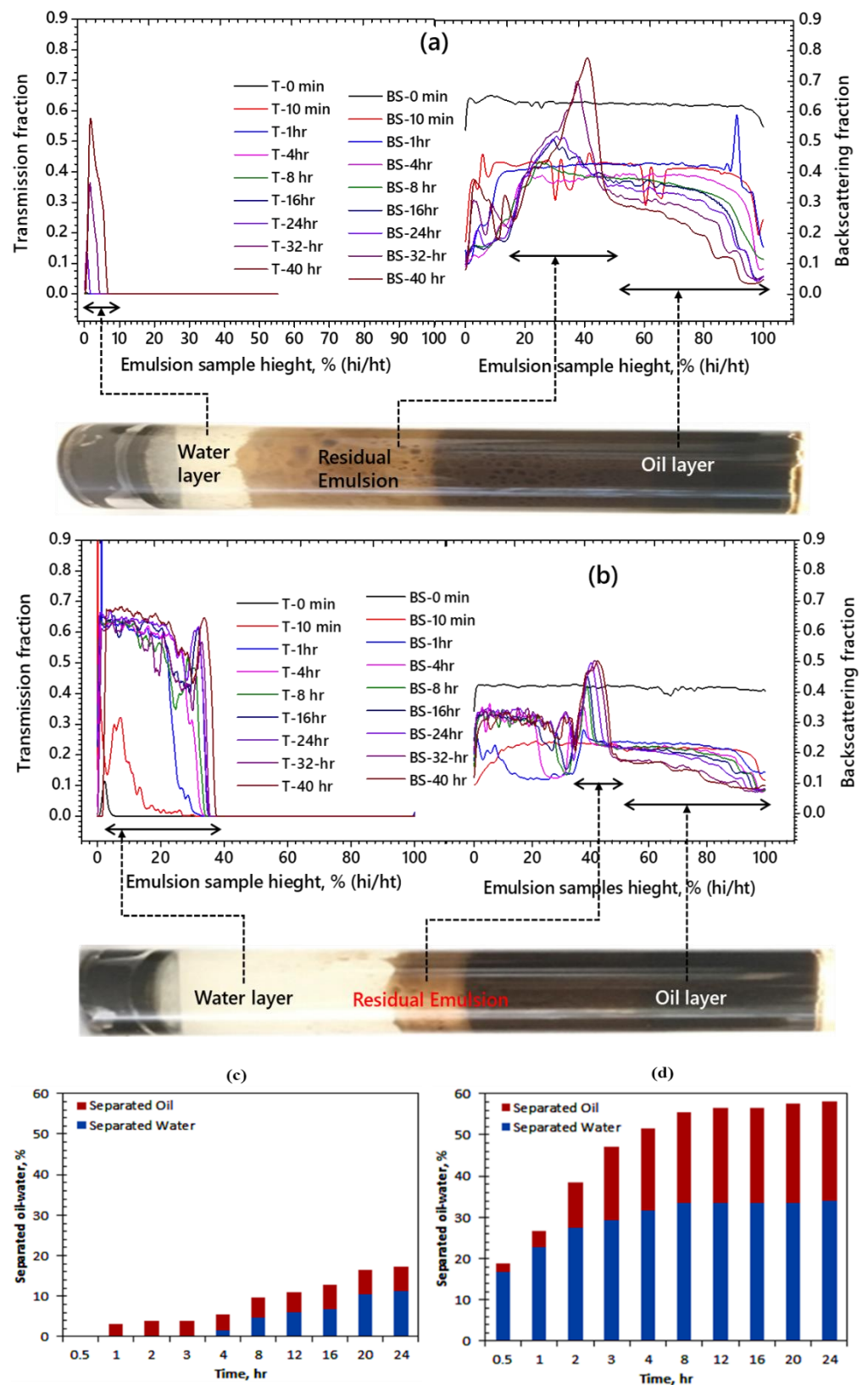


**Figure 5.** De-emulsification of ASP-produced emulsion (a) without  $\text{TiO}_2$  nanoparticles and (b) with  $\text{TiO}_2$  nanoparticles, and the percentage of oil/water separation (c) without  $\text{TiO}_2$  nanoparticles and (d) with  $\text{TiO}_2$  nanoparticles.



Based on the sedimentation of the water phase and coalescence of the oil phase, the separation of each phase was calculated. It is estimated that after 24 h, without  $\text{TiO}_2$  nanoparticles, only 13% of the o/w separation is achieved, as shown in Figure 5c, unlike previous studies by Ye et al. [39], where no oil droplet floatation was observed. On the other hand, the o/w separation increased to 32% (Figure 5d) in the presence of  $\text{TiO}_2$  nanoparticles, suggesting that the nanoparticles promote the o/w separation in an ASP-produced emulsion. A 19% increase in oil/water separation in the presence of  $\text{TiO}_2$  nanoparticles indicates that the stability of the ASP-produced emulsion considerably decreased. Backscattering of light at 24 h intervals shows the final rag layer growth, which is 15 mm and 26 mm with and without  $\text{TiO}_2$  nanoparticles, respectively. The measurement of light scattering from the sample at 10 min interval shows that emulsion is physically unstable in the presence of  $\text{TiO}_2$  nanoparticles. In contrast, the settlement of water is detected at 1 h, which shows that the emulsion is stable without  $\text{TiO}_2$  nanoparticles. The clarity of the separated water is 45% without  $\text{TiO}_2$  nanoparticles and 75% with  $\text{TiO}_2$  nanoparticles. In the presence of  $\text{TiO}_2$  nanoparticles, there is a significant positive effect on o/w separation and the separated water clarity. The results of o/w separation, residual emulsion layer, and rag layer formation are further visualized in Figure 6. It can be observed that the water layer in ASP-produced emulsion is small, whereas the rag layer and the oil layer are large without  $\text{TiO}_2$  nanoparticles. In contrast, the water layer increased while a momentous decrease in rag layer growth is observed in the presence of  $\text{TiO}_2$  nanoparticles. It can be concluded that the addition of  $\text{TiO}_2$  nanoparticles significantly improved the o/w separation indicated by the higher transmission and low backscattering by the ASP produced emulsion in Figure 4a,b.

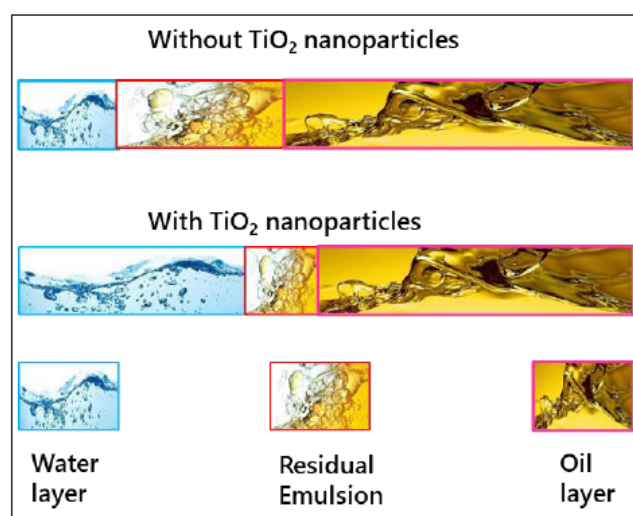


**Figure 6.** Schematic diagram of the de-emulsification of ASP-produced emulsion without  $\text{TiO}_2$  nanoparticles and with  $\text{TiO}_2$  nanoparticles and water, rag, and oil layer formation.

### 3.3. Droplet Size and Zeta Potential of Emulsion with and without $\text{TiO}_2$ Nanoparticle

In the following section, droplet size and zeta potential measurements of various emulsions with and without  $\text{TiO}_2$  are presented. The median diameter of the oil droplet before and after the addition of  $\text{TiO}_2$  nanoparticles is shown in Figure 7a,b, respectively. Investigating the effect of  $\text{TiO}_2$  nanoparticles on the oil droplet size, 300 mg/L of  $\text{TiO}_2$  nanoparticles is added to the ASP-produced emulsion. An observable difference between the water droplet size before and after the addition of  $\text{TiO}_2$  nanoparticles is visible, where the water droplet size increased from 3  $\mu\text{m}$  to 35  $\mu\text{m}$ . It shows that as the alkali concentration varied, the droplet size insignificantly increased from 3.51  $\mu\text{m}$  to 5.59  $\mu\text{m}$ , with a standard deviation of 1.39  $\mu\text{m}$ . In contrast, a significant increase in the droplet size is recorded with the presence of  $\text{TiO}_2$  nanoparticles in the same compositions of emulsifiers in the crude emulsion. The significant increase in the oil droplet size indicates that the

ASP-produced emulsion had become unstable in the presence of  $\text{TiO}_2$  nanoparticles. There is a flocculence of droplets resulting in the coalescence of water drops with a mean drop size of  $35\ \mu\text{m}$  and a standard deviation of  $4.06\ \mu\text{m}$ . The results suggest that the emulsion becomes unstable in the presence of  $\text{TiO}_2$  nanoparticles. Once  $\text{TiO}_2$  is added into the emulsified oily wastewater, the coalescence behavior of the adjacent small oil droplets takes place rapidly to form a big-sized oil droplet, as shown in Figure 7b. Thus, the oil aggregation forms the micro-clusters and then the micro-clusters are aggregated quickly to form macro clusters and float up to form the oil phase. Such findings indicate that the  $\text{TiO}_2$  acts as a de-emulsifier and improves the coalescence ability of adjacent small oil droplets in the emulsified oily wastewater when they contact each other.

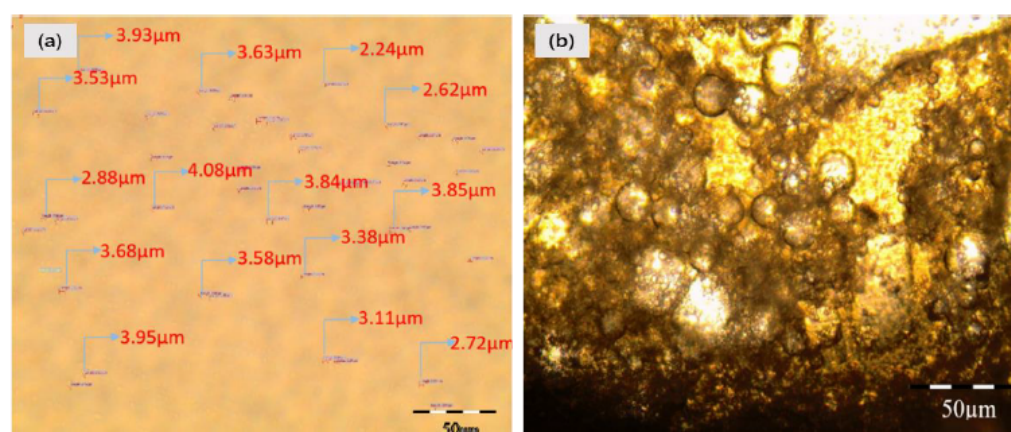


**Figure 7.** Cross polarized microscope (CPM) images of emulsions with and without  $\text{TiO}_2$  nanoparticles; (a) CPM image of emulsion in the presence of Alkali: 500; Surfactant: 400 ppm; Polymer: 600 ppm; (b) CPM image of emulsion in the presence of Alkali: 500; Surfactant: 400 ppm; Polymer: 600 ppm and  $\text{TiO}_2$  nanoparticles.

A similar trend of zeta potential was also noticed and in the presence of  $\text{TiO}_2$  nanoparticles, and the droplet zeta potential is in the unstable emulsion range as shown in Figure 8b. The zeta potential of the emulsion before the addition of  $\text{TiO}_2$  nanoparticles was  $-13\ \text{mV}$ , which suggests that the water droplets have a greater electrostatic repulsion. It has been reported elsewhere that the greater the electrostatic repulsion, the slimmer the possibility of the coalescence between the oil droplets [40].

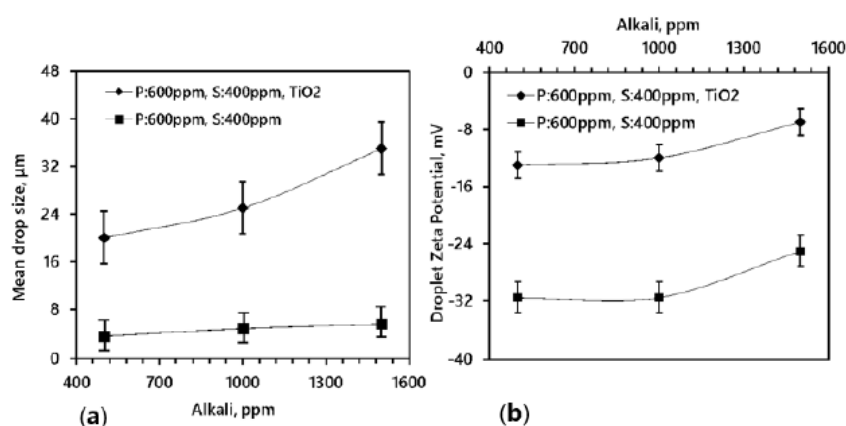


**Figure 8.** Droplet size and zeta potential before and after treatment with  $\text{TiO}_2$  (a) Mean drop size of 5 and  $35\ \mu\text{m}$  determined with a cross-polarized microscope at various ASP concentrations and 40% water cut with and without  $\text{TiO}_2$ , respectively. (b) Droplets Zeta Potential (attraction force) at various ASP concentrations and 40% water cut with and without  $\text{TiO}_2$ .

The present study shows that the zeta potential remains almost the same in the range of 500 to 1000 ppm of alkali. Likewise, an earlier study also showed that the zeta potential of the droplets increases after 800 ppm of alkali [41]. With the increasing polymer, the zeta potential ranges significantly from  $-20$  mV to  $-35$  mV and remains the same at the high water cut [42]. Importantly, when the  $\text{TiO}_2$  nanoparticles were added to the emulsion, the zeta potential of the residual emulsion increases to  $-7$  mV, which indicates the charge neutralization in the system and is advantageous for better o/w separation in the emulsion.  $\text{TiO}_2$  nanoparticles shrink the electrostatic repulsion obstacle in the ASP-produced emulsion, improving the oil droplets' chances of coalescing easily.

### 3.4. De-Stabilization of Emulsion

The plausible mechanism of the o/w separation in the presence of  $\text{TiO}_2$  nanoparticles can be explained based on the literature. The addition of  $\text{TiO}_2$  nanoparticles to the ASP-produced emulsion reduces the surface tension, making the oil droplets move to the hydrophilic surface of the  $\text{TiO}_2$ . In this way, many oil molecules can be trapped on the surface of  $\text{TiO}_2$  [43], and the water droplet is destabilized due to a decrease in the strength of the interfacial film. Simultaneously, the  $\text{TiO}_2$  has neutralized the charge present on the surface of the water drop, resulting in the reduction of the repulsive forces between them and promoting their coalescence. Neutralization of the charge by  $\text{TiO}_2$  flocculants govern the de-emulsification of water drops and their aggregate formation. The small oil droplets stick together to form larger droplets, resulting in their separation by the gravitational force. Afterwards, in the presence of  $\text{TiO}_2$  nanoparticles, the residual oil separates from the water phase, which is in good agreement with the previous studies [44]. Based on the previous literature, it can be inferred that the small emulsified droplets were captured, coalesced and detached, which turned the emulsified o/w mixture into a stratified one in the presence of  $\text{TiO}_2$  nanoparticles [45]. It can be concluded that since  $\text{TiO}_2$  is hydrophilic, it selectively adsorbs water from the o/w mixture, thus increasing the o/w separation. This consideration is supported by an earlier study, which confirmed that emulsified droplets in the continuous phase coalesce readily on favorable hydrophilic surfaces such as  $\text{TiO}_2$  [46]. It was also reported that two droplets coalesce easily on a hydrophilic surface within 20 s. Because, in the present work, the  $\text{TiO}_2$  nanoparticles are studied in a dispersed form, it is difficult to measure the contact angle to determine the degree of hydrophilicity. To quantify the degree of hydrophilicity and its effect on o/w separation, the  $\text{TiO}_2$  nanoparticles need to be coated on a substrate to make the contact angle measurements possible. Future work is necessary to confirm the exact mechanism of o/w separation in the presence of  $\text{TiO}_2$  nanoparticles, proposed here, by measuring the contact angle. ASP-produced water contains a large amount of inorganic salts, which shield the electrostatic repulsion between the surfactant ion head groups [47]. After the surfactant is removed from the oil and water interface, it goes to the water phase and various techniques are being used to remove the surfactant from the separated water phase [48].

## 4. Conclusions

The present study investigated the impact of  $\text{TiO}_2$  nanoparticles on the de-stabilization of enhanced oil recovery (EOR) which produced a stable emulsion. The anatase phase  $\text{TiO}_2$  nanoparticles with spherical morphology and an average particle size of 122 nm is synthesized via the chemical precipitation technique. The addition of  $\text{TiO}_2$  nanoparticles has a profound impact on o/w separation in an ASP-produced stable emulsion. The light transmission and backscattering measurements reveal enhanced o/w separation in an ASP-produced stable emulsion in the presence of  $\text{TiO}_2$  nanoparticles, while only flooding of ASP emulsion resulted in a lower o/w separation. The light transmission was enhanced from 50% to 68% without and in the presence of  $\text{TiO}_2$  nanoparticles, respectively. The o/w separation was only 13% without  $\text{TiO}_2$  nanoparticles, while an increment of 19% is achieved in the presence of  $\text{TiO}_2$  nanoparticles. This can be attributed to the improved coalescence action between the adjacent oil droplets and the improved behavior of the

oil/water interfacial film in the presence of TiO<sub>2</sub> nanoparticles. A clearly observable difference was found between the water droplet size before and after the addition of TiO<sub>2</sub> nanoparticles, where the water droplet size was increased from 3 µm to 35 µm. A similar trend of zeta potential has been noticed, showing that, with the presence of TiO<sub>2</sub> nanoparticles, the droplet zeta potential is in the unstable emulsion range. The emulsion's zeta potential before the addition of TiO<sub>2</sub> nanoparticles was −13 mV, which suggests that the oil droplets have a higher electrostatic repulsion. The results indicate a significant impact of TiO<sub>2</sub> nanoparticles on the stability of ASP-produced emulsion, and the addition of TiO<sub>2</sub> nanoparticles considerably destabilized the emulsion. The TiO<sub>2</sub> has contributed as flocculants that govern the de-emulsification of water droplets by charge neutralization. Future study is recommended to investigate the effect of particle size and morphology of TiO<sub>2</sub> nanoparticles on the destabilization of the EOR-produced emulsion.

**Author Contributions:** J.A.K. performed the project administration, funding acquisition, supervision, literature review, paper drafting and conceptualization. M.K.A.K. performed the project management, paper drafting, paper review and funding acquisition. S.I. contributed to the article writing, structuring and review of results, resources, and visualization. M.I. performed the literature review, and the article review. H.U. performed characterization. H.H.A.-K. performed review of the article. W.G., H.L. and S.R. performed the extensive review and resource management. A.G. performed draft review, technical expertise, and fund management. All authors have read and agreed to the published version of the manuscript.

**Funding:** The journal fee was paid by AGH University of Science and Technology, through grant No. 16.16.120.773.

**Institutional Review Board Statement:** Not applicable.

**Informed Consent Statement:** Not applicable.

**Data Availability Statement:** Not applicable.

**Acknowledgments:** The authors acknowledge the financial support from the Ministry of Education, Saudi Arabia and the Deanship of Scientific Research, Najran University, Saudi Arabia, under the grant code number NU/ESCI/17/066. The authors also acknowledge Universiti Teknologi PETRONAS Malaysia and Nazarbayev University, Nur-Sultan City, Kazakhstan for the technical support and data resources.

**Conflicts of Interest:** The authors declare no conflict of interest.

## References

1. Elanchezhian, S.S.; Prabhu, S.M.; Meenakshi, S. Effective adsorption of oil droplets from oil-in-water emulsion using metal ions encapsulated biopolymers: Role of metal ions and their mechanism in oil removal. *Int. J. Biol. Macromol.* **2018**, *112*, 294–305. [\[CrossRef\]](#) [\[PubMed\]](#)
2. Khan, J.; Al-Kayiem, H.; Aris, M. Stabilization of Produced Crude Oil Emulsion in the Presence of ASP. In Proceedings of the SPE Asia Pacific Enhanced Oil Recovery Conference, Kuala Lumpur, Malaysia, 11–13 August 2015.
3. Li, J.X.; Liu, Y.; Wu, D.; Meng, X.C.; Zhao, F.L. The synergistic effects of alkaline, surfactant, and polymer on the emulsification and destabilization of oil-in-water crude oil emulsion produced by alkaline-surfactant-polymer flooding. *Pet. Sci. Technol.* **2013**, *31*, 399–407. [\[CrossRef\]](#)
4. Kudaibergenov, S.; Akhmedzhanov, T.; Zhappasbayev, B.Z.; Gussenov, I.S.; Shakhvorostov, A.J.I.J.C.S. Laboratory study of ASP flooding for viscous oil. *Inter. J. Chem. Sci.* **2015**, *13*, 2017–2025.
5. Norrman, K.; Olesen, K.B.; Zimmermann, M.S.; Fadhel, R.; Vijn, P.; Sølling, T.I. Isolation and Characterization of Surface-Active Components in Crude Oil—Toward Their Application as Demulsifiers. *Energy Fuels* **2020**, *34*, 13650–13663. [\[CrossRef\]](#)
6. Yang, F.; Tchoukov, P.; Qiao, P.; Ma, X.; Pensini, E.; Dabros, T.; Czarnecki, J.; Xu, Z. Studying demulsification mechanisms of water-in-crude oil emulsions using a modified thin liquid film technique. *Colloids Surf. A Physicochem. Eng. Asp.* **2018**, *540*, 215–223. [\[CrossRef\]](#)
7. Demirbas, A.; Bamufleh, H.S.; Edris, G.; Alalayah, W.M. Treatment of contaminated wastewater. *Pet. Sci. Technol.* **2017**, *35*, 883–889. [\[CrossRef\]](#)
8. Dickhout, J.M.; Moreno, J.; Biesheuvel, P.; Boels, L.; Lammertink, R.G.; de Vos, W.M. Produced water treatment by membranes: A review from a colloidal perspective. *J. Colloid Interface Sci.* **2017**, *487*, 523–534. [\[CrossRef\]](#)
9. Ran, J.; Liu, J.; Zhang, C.; Wang, D.; Li, X. Experimental investigation and modeling of flotation column for treatment of oily wastewater. *Int. J. Min. Sci. Technol.* **2013**, *23*, 665–668. [\[CrossRef\]](#)



10. Rajak, V.; Kumar, S.; Thombre, N.; Mandal, A. Synthesis of activated charcoal from saw-dust and characterization for adsorptive separation of oil from oil-in-water emulsion. *Chem. Eng. Commun.* **2018**, *205*, 897–913. [\[CrossRef\]](#)
11. Rajak, V.; Relish, K.; Kumar, S.; Mandal, A. Mechanism and kinetics of separation of oil from oil-in-water emulsion by air flotation. *Pet. Sci. Technol.* **2015**, *33*, 1861–1868. [\[CrossRef\]](#)
12. Huang, B.; Li, X.; Zhang, W.; Fu, C.; Wang, Y.; Fu, S. Study on Demulsification-Flocculation Mechanism of Oil-Water Emulsion in Produced Water from Alkali/Surfactant/Polymer Flooding. *Polymers* **2019**, *11*, 395. [\[CrossRef\]](#)
13. Van der Zande, M.J.; Muntinga, J.H.; Van den Broek, W. Emulsification of Production Fluids in the Choke Valve. In Proceedings of the SPE Annual Technical Conference and Exhibition, New Orleans, LA, USA, 27 September 1998.
14. Skjefstad, H.S.; Dudek, M.; Øye, G.; Stanko, M. The effect of upstream inlet choking and surfactant addition on the performance of a novel parallel pipe oil–water separator. *J. Pet. Sci. Eng.* **2020**, *189*, 106971. [\[CrossRef\]](#)
15. Deng, S.; Yu, G.; Jiang, Z.; Zhang, R.; Ting, Y.P. Destabilization of oil droplets in produced water from ASP flooding. *Colloids Surf. A Physicochem. Eng. Asp.* **2005**, *252*, 113–119. [\[CrossRef\]](#)
16. Chu, Z.; Feng, Y.; Seeger, S. Oil/water separation with selective superantwetwetting/superwetting surface materials. *Angew. Chem. Int. Ed.* **2015**, *54*, 2328–2338. [\[CrossRef\]](#)
17. Doshi, B.; Sillanpää, M.; Kalliola, S. A review of bio-based materials for oil spill treatment. *Water Res.* **2018**, *135*, 262–277. [\[CrossRef\]](#)
18. Wang, C.-F.; Yang, S.Y.; Kuo, S.W. Eco-friendly superwetting material for highly effective separations of oil/water mixtures and oil-in-water emulsions. *Sci. Rep.* **2017**, *7*, 1–9.
19. Aleem, W.; Mellon, N.; Khan, J.A.; Al-Kayiem, H.H. Experimental investigation and mathematical modeling of oil/water emulsion separation effectiveness containing alkali-surfactant-polymer. *J. Dispers. Sci. Technol.* **2020**, 1–13. [\[CrossRef\]](#)
20. Khan, J.A.; Irawan, S.; Thurai, A.S.; Cai, B. Quantitative Analysis of Blowout Preventer Flat Time for Well Control Operation: Value Added Data Aimed at Performance Enhancement. *Eng. Fail. Anal.* **2020**, *120*, 104982. [\[CrossRef\]](#)
21. Khan, J.A.; Irfan, M.; Irawan, S.; Yao, F.K.; Abdul Rahaman, M.S.; Shahari, A.R.; Glowacz, A.; Zeb, N. Comparison of Machine Learning Classifiers for Accurate Prediction of Real-Time Stuck Pipe Incidents. *Energies* **2020**, *13*, 3683. [\[CrossRef\]](#)
22. Khalilnezhad, A.; Rezvani, H.; Ganji, P.; Kazemzadeh, Y. A Complete Experimental Study of Oil/Water Interfacial Properties in the Presence of TiO<sub>2</sub> Nanoparticles and Different Ions. *Oil Gas Sci. Technol.-Rev. d'IFP Energ. Nouv.* **2019**, *74*, 39. [\[CrossRef\]](#)
23. Shi, B.; Jia, X.; Guo, Z. An easy preparation of photo-response TiO<sub>2</sub>@copper wire mesh with quick on/off switchable superwetting for high efficiency oil–water separation. *New J. Chem.* **2018**, *42*, 17563–17573. [\[CrossRef\]](#)
24. Cheraghian, G. Effects of titanium dioxide nanoparticles on the efficiency of surfactant flooding of heavy oil in a glass micromodel. *Pet. Sci. Technol.* **2016**, *34*, 260–267. [\[CrossRef\]](#)
25. Cheraghian, G. Effect of nano titanium dioxide on heavy oil recovery during polymer flooding. *Pet. Sci. Technol.* **2016**, *34*, 633–641. [\[CrossRef\]](#)
26. Hassan, Y.M.; Guan, B.H.; Zaid, H.M.; Hamza, M.F.; Adil, M.; Adam, A.A.; Hastuti, K. Application of Magnetic and Dielectric Nanofluids for Electromagnetic-Assistance Enhanced Oil Recovery: A Review. *Crystals* **2021**, *11*, 106. [\[CrossRef\]](#)
27. Shah, R.D. Application of Nanoparticle Saturated Injectant Gases for EOR of Heavy Oils. In Proceedings of the SPE Annual Technical Conference and Exhibition, New Orleans, LA, USA, 4 October 2009.
28. Ehtesabi, H.; Ahadian, M.M.; Taghikhani, V.; Ghazanfari, M.H. Enhanced heavy oil recovery in sandstone cores using TiO<sub>2</sub> nanofluids. *Energy Fuels* **2014**, *28*, 423–430. [\[CrossRef\]](#)
29. Khan, J.A.; Al-Kayiem, H.H.; Aleem, W.; Saad, A.B. Influence of alkali-surfactant-polymer flooding on the coalescence and sedimentation of oil/water emulsion in gravity separation. *J. Pet. Sci. Eng.* **2019**, *173*, 640–649. [\[CrossRef\]](#)
30. Al-Kayiem, H.H.; Khan, J.A. Evaluation of Alkali/Surfactant/Polymer Flooding on Separation and Stabilization of Water/Oil Emulsion by Statistical Modelling. *Energy Fuels* **2017**, *31*, 9290–9301. [\[CrossRef\]](#)
31. Schramm, L.L. Emulsions: Fundamentals and applications in the petroleum industry. *Adv. Chem.* **1992**, *231*, 3–24.
32. Kokal, S.L. Crude oil emulsions: A state-of-the-art review. *SPE Prod. Facil.* **2005**, *20*, 5–13. [\[CrossRef\]](#)
33. Li, J.-G.; Ishigaki, T.; Sun, X. Anatase, brookite, and rutile nanocrystals via redox reactions under mild hydrothermal conditions: Phase-selective synthesis and physicochemical properties. *J. Phys. Chem. C* **2007**, *111*, 4969–4976. [\[CrossRef\]](#)
34. Mostaghni, F.; Abed, Y. Structural determination of Co/TiO<sub>2</sub> nanocomposite: XRD technique and simulation analysis. *Mater. Sci. Poland* **2016**, *34*, 534–539. [\[CrossRef\]](#)
35. Yahaya, M.Z.; Azam, M.A.; Teridi, M.A.M.; Singh, P.K.; Mohamad, A.A. Recent Characterisation of Sol-Gel Synthesised TiO<sub>2</sub> Nanoparticles. *Recent Appl. Sol-Gel Synth.* **2017**. [\[CrossRef\]](#)
36. Choi, S.K.; Son, H.A.; Kim, H.T.; Kim, J.W. Nanofluid enhanced oil recovery using hydrophobically associative zwitterionic polymer-coated silica nanoparticles. *Energy Fuels* **2017**, *31*, 7777–7782. [\[CrossRef\]](#)
37. Kameya, Y.; Yabe, H. Optical and superhydrophilic characteristics of TiO<sub>2</sub> coating with subwavelength surface structure consisting of spherical nanoparticle aggregates. *Coatings* **2019**, *9*, 547. [\[CrossRef\]](#)
38. Kang, W.; Guo, L.; Fan, H.; Meng, L.; Li, Y. Flocculation, coalescence and migration of dispersed phase droplets and oil–water separation in heavy oil emulsion. *J. Pet. Sci. Eng.* **2012**, *81*, 177–181. [\[CrossRef\]](#)
39. Ye, F.; Wang, Z.; Mi, Y.; Kuang, J.; Jiang, X.; Huang, Z.; Luo, Y.; Shen, L.; Yuan, H.; Zhang, Z.J.C.; et al. Preparation of reduced graphene oxide/titanium dioxide composite materials and its application in the treatment of oily wastewater. *Colloids Surfaces* **2020**, *586*, 124251. [\[CrossRef\]](#)



40. Bi, Y.; Li, W.; Liu, C.; Xu, Z.; Jia, X.J.E. Dendrimer-based demulsifiers for polymer flooding oil-in-water emulsions. *Energy Fuels* **2017**, *31*, 5395–5401. [[CrossRef](#)]
41. Di, W.; Meng, X.; Zhao, F.; Zhang, R.; Yan, C.; Wang, Q.; Liang, H. Emulsification and Stabilization of ASP Flooding Produced Liquid. In Proceedings of the SPE International Symposium on Oilfield Chemistry, Houston, TX, USA, 8 March 2015.
42. Yang, L.; Wang, Z.; Zhuge, X.; Wang, S. Study on Emulsification Behavior and Optimized Separation Technology of High Concentration Polymer Flooding Produced Liquid in Daqing Oilfield. In Proceedings of the SPE Middle East Oil & Gas Show and Conference, Manama, Bahrain, 18–21 March 2019.
43. Liang, H.; Esmaili, H. Application of nanomaterials for demulsification of oily wastewater: A review study. *Environ. Technol. Innov.* **2021**, *22*, 101498. [[CrossRef](#)]
44. Goh, P.S.; Ong, C.S.; Ng, B.C.; Ismail, A.F. 5—Applications of Emerging Nanomaterials for Oily Wastewater Treatment. In *Nanotechnology in Water and Wastewater Treatment*; Ahsan, A., Ismail, A.F., Eds.; Elsevier: Amsterdam, The Netherlands, 2019; pp. 101–113. [[CrossRef](#)]
45. Chen, C.; Weng, D.; Mahmood, A.; Chen, S.; Wang, J. Separation mechanism and construction of surfaces with special wettability for oil/water separation. *ACS Appl. Mater. Interfaces* **2019**, *11*, 11006–11027. [[CrossRef](#)]
46. Li, Y.; Cao, L.; Hu, D.; Yang, C. Uncommon wetting on a special coating and its relevance to coalescence separation of emulsified water from diesel fuel. *Sep. Purif. Technol.* **2017**, *176*, 313–322. [[CrossRef](#)]
47. Zhang, D.; Chen, Z.; Ren, L.; Meng, X.; Gu, W. Study on stability of produced water in ASP flooding based on critical micellar theory. *Polym. Bull.* **2020**, 1–14.
48. Krishnan, S.; Chandran, K.; Sinnathambi, C.M. Wastewater Treatment Technologies Used for the Removal of Different Surfactants: A Comparative. *Int. J. Appl. Chem.* **2016**, *12*, 727–739.